

SPACE ASTROMETRY OF THE VERY MASSIVE $\sim 150 M_{\odot}$ RUNAWAY STAR CANDIDATE VFTS682

M. RENZO^{*1}, S. E. DE MINK¹, D. J. LENNON², I. PLATAIS³, R. P. VAN DER MAREL^{3,4}, E. LAPLACE¹, J. M. BESTENLEHNER⁵, C. J. EVANS⁶, V. HÉNAULT-BRUNET⁷, S. JUSTHAM^{1,8,9}, A. DE KOTER¹, N. LANGER¹⁰, F. NAJARRO¹¹, H. SANA¹², F. R. SCHNEIDER¹³, J. S. VINK¹⁴

* Corresponding author: m.renzo@uva.nl. A list of the affiliations can be found at the end of this paper.

Draft version August 21, 2018

ABSTRACT

How very massive stars form is still an intriguing open question in stellar astrophysics. VFTS682 is among the most massive stars known, with an inferred initial mass of $\sim 150 M_{\odot}$. It is located in 30 Doradus at a projected distance of 29 pc from the central cluster R136. The absence of other massive stars in its immediate vicinity led to two intriguing hypotheses: either (a) it formed in relative isolation or (b) it was ejected dynamically from the central cluster.

In this context, we investigate the kinematics of VFTS682 as obtained by *Gaia* and multi-epoch *Hubble Space Telescope* photometry. We derive a projected velocity relative to the cluster of $\sim 30 \pm 20 \text{ km s}^{-1}$ at one σ level. The direction and magnitude of the proper motion are consistent with VFTS682 being a slow runaway ejected from the central cluster, given its distance and the inferred age. However, the error bars are substantial and the proper motion measurements alone cannot rule out the counter hypothesis with high confidence.

If future data confirm the runaway nature, this would make the VFTS682 the most massive runaway star known to date. While we cannot prove this solidly from the current data alone, we do consider this hypothesis as the most plausible because of a variety of circumstantial clues. The central cluster is known to harbor several other stars more massive than $150 M_{\odot}$ of similar in spectral type. The very massive O stars VFTS16 and VFTS72, which have recently been identified as a dynamically ejected runaway, provides direct evidence that R136 is indeed capable of ejecting some of its most massive members, consistent with the predictions of numerical simulations.

Subject headings: stars: kinematics, stars: runaways, stars: individual: VFTS682

1. INTRODUCTION

How massive stars form is one of the major longstanding questions in astrophysics (e.g., Zinnecker & Yorke 2007). Improving our understanding of massive star formation, and its possible dependence on environment and metallicity, is crucial for understanding the role massive stars play within their host galaxies, but also for understanding the transients that mark their death and the compact remnants they leave behind. Obtaining clues from observations is challenging, because massive stars are intrinsically rare, evolve fast, typically reside in dense groups, and remain enshrouded in their parent cloud during the entirety of the formation process. Important progress has been made on the theoretical side, (e.g. Bate 2009; Kuiper et al. 2015; Rosen et al. 2016), but the simulations of this multi-scale and multi-physics problem are computationally expensive and remain challenging.

It has been proposed that most, if not all, stars form in clusters (Lada & Lada 2003), where massive stars are thought to reside in the innermost cores. In this picture, field stars are primarily the result of the dissolution of dense groups. However, a significant population of massive stars exists in relative isolation, far from dense clusters or OB associations and their origin remains matter of debate (Gvaramadze et al. 2012; Lamb et al. 2016; Ward & Kruijssen 2018). One hypothesis to explain the population of relatively isolated massive stars is that they formed in the field. The alternative hypothesis is that these massive stars were ejected from the clusters in which they formed. Such ejections may result from dynamical interactions (e.g., Poveda et al. 1967) or from the disruption of binary systems at the death of the companion star (e.g., Blaauw 1961; Renzo et al. 2018).

One of the most extreme examples that has been consid-

ered in this debate is the very massive star VFTS682 (Bestenlehner et al. 2011; Bressert et al. 2012). This star is located in the field of the 30 Doradus region in the Large Magellanic Cloud (LMC) and was studied as part of the multi-epoch spectroscopic VLT-FLAMES Tarantula Survey (VFTS, Evans et al. 2011). It is a hydrogen-rich Wolf-Rayet star of spectral type WN5. Spectral analysis and comparison with evolutionary models lead to an inferred present-day mass of $\sim 137.8^{+27.5}_{-15.9} M_{\odot}$ corresponding to an initial mass of $\sim 150.0^{+28.7}_{-17.4} M_{\odot}$ (Schneider et al. 2018). This makes VFTS682 one of the most massive stars known and one of the most extreme objects in the region. From the spectral point of view, it is reminiscent of the very massive stars in the core of the R136 cluster (de Koter et al. 1997; Crowther et al. 2010, 2016). In particular, a remarkable similarity exist between the spectrum of VFTS682 and R136a3 (Rubio-Díez et al. 2017).

VFTS682 stands out by its relative isolation at a projected distance of 119.4 arcseconds, corresponding to ~ 29 pc, from the star cluster R136. Bestenlehner et al. (2011) considered two possible explanation for the offset: either the star formed in situ as an isolated massive star, or it was ejected from R136. N-body simulations indicate that the ejection of very massive stars like VFTS682 is expected (e.g. Fujii & Portegies Zwart 2011; Banerjee et al. 2012). This is supported by the recent findings of other massive runaway stars in the region based on proper motion studies.

Platais et al. (2015, 2018) analyzed multi-epoch *Hubble Space Telescope* (HST) photometry and identified 10 stars likely ejected from R136. Lennon et al. (2018) investigate the kinematics of isolated O-type stars in the region using the second *Gaia* data release (DR2, Gaia Collaboration et al. 2016, 2018) and show that the proper motion, position and direction

TABLE 1
SELECTED STELLAR PARAMETERS FOR VFTS682.

| Parameter | Units | Value | Ref. |
|---|---------------------------------|-------------------------|------|
| <i>Selected stellar parameters VFTS 682</i> | | | |
| present day mass | [M_{\odot}] | $137.8^{+27.5}_{-15.9}$ | (1) |
| initial mass | [M_{\odot}] | $150.0^{+28.7}_{-17.4}$ | (1) |
| age | [Myr] | 1.0 ± 0.2 | (1) |
| mass loss rate | [$M_{\odot} \text{ yr}^{-1}$] | $10^{-4.1 \pm 0.2}$ | (2) |

NOTE. — The quoted errors are statistical, and do not include systematic effects in the modeling.

(1) Schneider et al. (2018) (2) Bestenlehner et al. (2011)

of the $\sim 100 M_{\odot}$ star VFTS16 is consistent with a runaway origin from R136. They also found a less clear case for VFTS72, and in both cases some tension between the kinematic age of these stars and their apparent age remains.

In this paper we present an analysis of the new kinematical constraints for VFTS682 provided by *Gaia* DR2 and constraints from HST proper motions by Platais et al. (2018). We discuss the implications for the hypothesis that VFTS682 is a slow runaway star ejected from R136.

2. OBSERVATIONS

The WNh5 star VFTS682, located at right ascension (RA) $05^{\text{h}}38^{\text{m}}55.510^{\text{s}}$ and declination (DEC) $-69^{\circ}04'26.72''$ J2000, was observed as part of the multi-epoch, spectroscopic VFTS campaign covering $\lambda 4000\text{--}7000$ (Evans et al. 2011). Bestenlehner et al. (2011) analyzed the spectra to infer the stellar parameters and measure an extinction of $A_V = 4.45 \pm 0.12$, implying a luminosity of $\log_{10}(L/L_{\odot}) = 6.5 \pm 0.2$, making this one of the brightest stars in the region. The absence of radial velocity variations suggests that the star is unlikely to have close binary companions Bestenlehner et al. (2011), unless the orbital inclination is very high. Bayesian fits of the stellar parameters against evolutionary tracks (Brott et al. 2011; Köhler et al. 2015) using the BONNSAI code (Schneider et al. 2017, 2018) provide estimates for the age, present mass and initial mass, Table 1.

Townsley et al. (2006) did not find a bright X-ray point source at the position of VFTS682 in their *Chandra* survey of the region, which suggests the absence of colliding winds that would be expected in the presence of companions even for extreme mass ratios, given the extremely large mass of VFTS682. This star is also relatively isolated in (near) infrared. There nearest bright (near-)infrared sources detected by *Spitzer* (Meixner et al. 2006) and resolved in the *VISTA* Magellanic Clouds Survey (Cioni et al. 2011) are located at a distance of about 10 arcsecond, i.e. about 2.4 pc. Walborn et al. (2013) speculate that these nearby young stars may represent a case of starformation triggered by the the wind of VFTS682, but chance alignment cannot be excluded.

The V-band light curve of VFTS682 shows variations at a $\sim 10\%$ level on a timescale of years, which is unusual for Wolf-Rayet stars and more typical for Luminous Blue Variable (LBV) stars (Udalski et al. 2008; Bestenlehner et al. 2011). It also shows mid-infrared excess (Gruendl & Chu 2009).

Estimates of the radial velocity are complicated by the variable, possibly inhomogeneous, optically thick wind typical of emission line stars. Bestenlehner et al. (2011) estimate a mass loss rate of $10^{-4.1 \pm 0.2} M_{\odot} \text{ yr}^{-1}$, not accounting for the possible effect of clumping. We therefore caution for over-interpreting

TABLE 2
KINEMATICS OF VFTS682.

| Parameter | Units | Value | Ref. |
|--|-------------------|-------------------|--------|
| <i>Absolute and relative position</i> | | | |
| RA _{VFTS682} | [degrees] | 84.7314 | (1) |
| DEC _{VFTS682} | [degrees] | -69.0741 | (1) |
| RA _{R136} | [degrees] | 84.6767 | SIMBAD |
| DEC _{R136} | [degrees] | -69.1009 | SIMBAD |
| δRA | [mas sec] | 0.0547 | (2, 5) |
| δDEC | [mas sec] | 0.0268 | (2, 5) |
| d_{\parallel} | [arcsec] | 119.4 | SIMBAD |
| L_{\parallel} | [pc] | 29 | (2) |
| <i>Gaia absolute proper motion for VFTS682 and the region</i> | | | |
| μ_{RA} | [mas yr $^{-1}$] | 1.843 ± 0.070 | (1) |
| μ_{DEC} | [mas yr $^{-1}$] | 0.786 ± 0.080 | (1) |
| $\rho(\mu_{\text{RA}}, \mu_{\text{DEC}})$ | [mas yr $^{-1}$] | 0.0226 | (1) |
| $\langle \mu_{\text{RA}} \rangle_{\text{R136}}$ | [mas yr $^{-1}$] | 1.74 ± 0.01 | (3) |
| $\langle \mu_{\text{DEC}} \rangle_{\text{R136}}$ | [mas yr $^{-1}$] | 0.70 ± 0.02 | (3) |
| <i>Gaia relative proper motion for VFTS682</i> | | | |
| $\delta\mu_{\text{RA}}$ | [mas yr $^{-1}$] | 0.103 ± 0.080 | (1, 5) |
| $\delta\mu_{\text{DEC}}$ | [mas yr $^{-1}$] | 0.086 ± 0.100 | (1, 5) |
| $\delta\mu_{\text{Gaia}}$ | [mas yr $^{-1}$] | 0.13 ± 0.09 | (1, 5) |
| v_{2d} | [km s $^{-1}$] | 32 ± 21 | (1, 5) |
| θ_{Gaia} | [degrees] | 14^{+36}_{-31} | (1, 5) |
| <i>HST relative proper motion for VFTS682</i> | | | |
| $\delta\mu_{\text{RA,HST}}$ | [mas yr $^{-1}$] | 0.01 ± 0.13 | (4) |
| $\delta\mu_{\text{DEC,HST}}$ | [mas yr $^{-1}$] | 0.20 ± 0.10 | (4) |
| $\delta\mu_{\text{HST}}$ | [mas yr $^{-1}$] | 0.20 ± 0.10 | (4) |
| $v_{2d,\text{HST}}$ | [km s $^{-1}$] | 47 ± 24 | (4) |
| θ_{HST} | [degrees] | -35^{+24}_{-51} | (1, 5) |
| <i>Expected proper motion if ejected from R136 at age zero</i> | | | |
| v_{2d} | [km s $^{-1}$] | 29 ± 6 | (2) |
| θ | [degrees] | ~ 0 | |

NOTE. — Proper motions are based on Gaia data unless indicated otherwise in subscript. The conversion factor assuming a distance of 50 kpc is such that 1 mas yr $^{-1}$ corresponds to 237 km s $^{-1}$. The correlation coefficient is indicated as ρ . The angle θ is defined such that $\theta = 0$ for motions pointing away radially from R136, we neglect the errors on $\langle \mu_{\text{RA}} \rangle_{\text{R136}}$ and $\langle \mu_{\text{DEC}} \rangle_{\text{R136}}$ to determine the uncertainty on θ_{Gaia} . (1) Gaia Collaboration et al. (2018), (2) Bestenlehner et al. (2011), (3) Lennon et al. (2018), (4) Platais et al. (2018) and (5) this study.

the estimates for the radial velocities. Bestenlehner et al. (2011) estimate a radial velocity (RV) of $300 \pm 10 \text{ km s}^{-1}$ using the Nv $\lambda 4944$ line, which is offset from the average radial velocity of the region of $270 \pm 10 \text{ km s}^{-1}$. This is consistent with, but no proof of, a runaway nature. Bressert et al. (2012) note an offset compared between the RV of the star and the nebular lines from the gas filaments in its vicinity. This is consistent with the expectation if the star was not formed in situ. Newer measurements based on new X-shooter data give different estimates for the RV (Rubio-Díez et al. in prep). We will therefore refrain from using the RV measurements in this work.

We adopt as distance to the LMC the value of 50 kpc. The error on the distance determination is small ($\lesssim 2\%$, Pietrzyński et al. 2013) and any possible offset in the radial direction between R136 or VFTS682 and the distance we adopted for the LMC is probably much smaller (likely $\ll 1\%$, e.g., Luks & Rohlfs 1992). These uncertainties are negligible compared to the errors in the proper motion discussed below.

2.1. Gaia astrometry for VFTS682

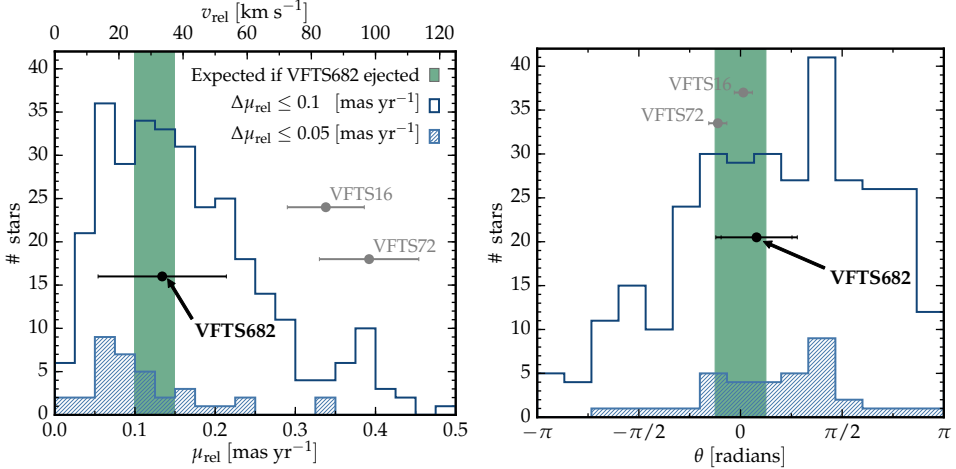


FIG. 1.— *Left panel:* distribution of OB-type and Wolf-Rayet stars in proper motion relative to R136. VFTS682 is not an outlier, but its relative proper motion matches the expected value if it were indeed ejected from R136 assuming an age of 1.0 ± 0.2 Myr. The top axis shows the conversion to physical units assuming a distance of 50 kpc. *Right panel:* distribution of angles between the relative proper motion direction and the radial direction from the center of the cluster to the star. The error bars from *Gaia* for VFTS682 are large, but the best value is in agreement with the hypothesis of dynamical ejection. The peak at $\theta \approx \pi/2$ is due to stars belonging to NGC2060. In both panels, the dark blue histograms contain 317 stars with error smaller than $0.1 \text{ mas yr}^{-1} \simeq 25 \text{ km s}^{-1}$ at 50 kpc, the lighter blue histograms contain 36 stars with errors smaller than 0.05 mas yr^{-1} .

VFTS682 is identified with the source id 4657685637907503744 in the *Gaia* DR2 catalog as a 15.65 mag star in the G band (Gaia Collaboration et al. 2016, 2018). The number of visibility periods, i.e., groups of observations separated from other groups by a gap of at least four days, used in the astrometric solution is seventeen for this star. The reported astrometric excess noise is zero. These values suggest that the *Gaia* DR2 data for VFTS682 are reliable.

Gaia provides absolute proper motions. To determine the relative proper motion with respect to R136, we follow Lennon et al. (2018) to define the motion of the local frame of reference using the average proper motion of nearby stars with reliable astrometric data. They selected bright ($G < 17$) stars within 0.05 degrees of R136 and exclude sources with proper motion errors greater than 0.01 mas yr^{-1} in both coordinates (see their Sect. 2.1).

With these we compute the relative proper motion $\delta\mu_{RA}$ and $\delta\mu_{DEC}$. We also compute the total projected 2d velocity v_{2d} and the angle θ between the direction of motion and the vector connecting the center of R136 with the current position of VFTS 682, i.e. such that $\theta = 0$ is the angle corresponding to perfectly radial motion away from R136. All kinematic quantities are provided in Table 2.

2.2. HST astrometry for VFTS682

The 30 Doradus region was target of an a two-epoch photometric campaign with HST providing observations in the F775W filter in October 2011 and October 2014 (GO-12499; P.I.: D. J. Lennon, Sabbi et al. 2013).

Platais et al. (2015, 2018) analyzed the HST data to determine the relative proper motion and identify candidate runaway stars. The brightest stars ($V < 14$) are saturated in the data set and have been excluded from the analysis. The high extinction around VFTS682 prevents this issue. VFTS682 is relatively slow and is therefore not discussed in their paper. However, their measurements are useful here, since they provides an estimate of the proper motion of VFTS682 that is independent from the *Gaia* measurement.

The HST provides proper motions that are relative to the bulk motion of the majority of the stars in the field of view.

The full 30 Dor field is covered by different pointings and there is some systematic distortion. However, even for stars far from 30 Dor the effect is small, no more than 0.05 mas yr^{-1} across the whole 30 Dor field. The effect is much smaller for stars close to the center of field, such as VFTS 682 (Platais et al. 2018). We can therefore use the relative proper motion (Table 2) as a good estimate for the proper motion relative to R136.

3. THE KINEMATICS OF VFTS682

The black points in Fig. 1 show the proper motion (left panel) and the projected flight direction (right panel) relative to R136 of VFTS682. θ is the angle between the projected radial direction from the center of R136 to each star and its projected relative proper motion (see also Fig. 2). Dynamical ejections from the cluster should produce close to radial ejections, i.e. $\theta \simeq 0$. The green vertical bands highlight the expectations for these two quantities if VFTS682 were ejected from R136 early in its lifetime. Although the error bars are substantial and VFTS682 is not an outlier, the agreement suggests that the star is indeed a “slow-runaway” as suggested by Bestenlehner et al. (2011). For comparison, we also show the relative proper motion of VFTS16 and VFTS72 (gray points), and the distribution in relative proper motion and flight direction for all the VFTS O/B-type and Wolf-Rayet stars with *Gaia* DR2 errors on the proper motion components of less than 0.1 mas yr^{-1} (dark blue lines, including VFTS682), and less than 0.05 mas yr^{-1} (light hatched blue).

Subtracting the mean motion of R136, we obtain relative proper motions (projected velocities) of $\delta\mu_{Gaia} = 0.13 \pm 0.09 \text{ mas yr}^{-1} (32 \pm 21 \text{ km s}^{-1})$ and $\delta\mu_{HST} = 0.20 \pm 0.10 \text{ mas yr}^{-1} (47 \pm 24 \text{ km s}^{-1})$. Both values are consistent with each other, but also with no relative motion within 2σ .

We note that VFTS72 has a small radial velocity, while VFTS16 (and possibly VFTS682) has large peculiar radial velocity and therefore accurate distances along the line of sight are needed to constrain the flight direction in three dimensions.

Figure 2 shows the projected motion of VFTS682 relative to R136 on the sky. We also show VFTS16 and VFTS72 for completeness (see Lennon et al. 2018). The thick yellow arrows are proportional to the relative proper motion from *Gaia*

DR2, and the thick green line illustrates the relative proper motion from HST. The error cone on the direction of motion is illustrated by the corresponding prolongation in the direction opposite to the motion, and we also show the most likely origin of the stars accounting for their apparent age. This figure illustrates that R136 is the most likely origin of these stars, although the large error bars prevent a robust identification for VFTS682, and there is some tension between the apparent age and the present day distance from the cluster core for VFTS16 and VFTS72 (Lennon et al. 2018).

Assuming VFTS682 indeed originates from R136, we can calculate its kinematic age simply as:

$$\tau_{\text{kin}} = \frac{d_{\parallel}}{\delta\mu_{\text{Gaia}}} \simeq \frac{119.4 \text{ arcsec}}{0.13 \text{ mas yr}^{-1}} \simeq 0.9 \pm 0.6 \text{ Myr} , \quad (1)$$

where $d_{\parallel} = 119.4 \text{ arcsec}$ is the angular distance from VFTS682 to the core of the cluster (corresponding to $\sim 29 \text{ pc}$ at a distance of 50 kpc , Bestenlehner et al. 2011). The kinematic age τ_{kin} is consistent with a very early ejection from the cluster, given the apparent age of the star.

In summary, both *Gaia* and HST relative proper motions are consistent with the dynamical ejection of VFTS682 from the cluster, although we cannot confidently rule out the counter hypothesis.

4. DISCUSSION

Based on our results, we consider likely that VFTS682 is the most massive (slow) runaway known to date, with a two-dimensional projected velocity with respect to R136 of $\sim 38 \text{ km s}^{-1}$ (averaging the *Gaia* DR2 and HST results), but compatible with zero within 2σ . Due to the large error bars, this result will need to be revisited with future astrometric data. If confirmed, it means that isolated star formation is *not* required to explain the isolation of VFTS682. Its proper motion suggests that it was ejected from the cluster R136 $0.9 \pm 0.6 \text{ Myr}$ ago. If the cluster age ($\lesssim 2 \text{ Myr}$, Crowther et al. 2010; Sabbi et al. 2012) is indeed smaller than the shortest stellar lifetime ($\sim 3 \text{ Myr}$, Brott et al. 2011; Zapartas et al. 2017), the ejection of VFTS682 from the disruption of a binary is excluded. The kinematic age we infer is smaller than the kinematic age of $\sim 1.5 \text{ Myr}$ for VFTS16 found in Lennon et al. (2018), which indicates that VFTS682 was ejected later than VFTS16, at a time similar to VFTS72.

If the star were ejected dynamically, its exceptionally large mass raises the question of which stars must populate the core of the cluster. N-body dynamics typically ejects the least massive star among those interacting (e.g., Banerjee et al. 2012). Just based on the kinematic properties of VFTS682, we would expect several stars with initial masses larger than $\sim 150 M_{\odot}$ in the cluster R136, which is consistent with the detection of extremely massive stars in the core of the cluster.

The spectral type of VFTS682 (WNh5, Bestenlehner et al. 2011) is the same as R136a1-a3, i.e. the three most massive stars detected in the core of the cluster, with an remarkable similarity in particular with the spectrum of R136a3. The isolation of VFTS682 makes it an ideal target to constrain the stellar physics of stars with masses well above $\sim 100 M_{\odot}$ while avoiding crowding issues.

The simulations of Fujii & Portegies Zwart (2011) suggest that early in the evolution of a cluster, dynamical interactions form an extremely massive binary, which then tightens its orbit by ejecting other stars. The spectral similarities between VFTS682 and stars in the core of R136 are in agreement with this “bully binary” model. Interpreting the kinematics of VFTS682 through the lens of their simulations suggests the presence of a close binary with total mass $M_1 + M_2 \gtrsim 300 M_{\odot}$ in the core of the cluster. The kinematic age of VFTS682 puts an upper limit to the timescale to form the “bully binary” in R136. Such binary could be R145 according to Fujii & Portegies Zwart (2011), and it might be an ideal observational candidate for a dynamically formed progenitor system of a binary black-hole, provided that stars this massive can avoid a pair-instability supernova (e.g., Rakavy & Shaviv 1967) at LMC metallicity (see also Langer et al. 2007).

Similarly, the final fate of VFTS682 could be either a pair-instability supernova without compact remnant formation, or possibly direct collapse to a black hole above the 2nd mass gap. The amount of mass loss of these stars will determine their final core mass and thus their final fate.

Also Banerjee et al. (2012) suggested, based on their N-body simulations, that VFTS682 was ejected from R136. In their model, they relied on (dynamically driven) stellar mergers to explain the high masses of VFTS682 and the massive members of R136. They demonstrated that the cluster potential does not significantly change the velocity of the star after the ejection. To eject such a massive object, the cluster is expected to have produced a large number of massive runaways. Indeed, several isolated massive stars are observed in the region (Evans et al. 2010; Lennon et al. 2018), some with known large radial velocities and/or proper motion. A comprehensive study of the kinematic properties of all the massive stars surrounding R136 could shed light on whether some can be unequivocally identified as merger products, but also on the initial conditions for the cluster dynamics (e.g., Oh & Kroupa 2016), and whether it formed via a monolithic collapse, or as a (potentially ongoing) merger of several sub-structures (e.g., Sabbi et al. 2012).

VFTS682 is potentially the most massive runaway known to date, and its ejection from the cluster R136 likely implies that it is only the “tip of the iceberg” of possibly extremely massive runaways in the region. Studies of this population, enabled by recent HST and *Gaia* observations will put constraints on the evolution of these extreme stars, together with the formation and evolution of the central cluster itself.

REFERENCES

- Banerjee, S., Kroupa, P., & Oh, S. 2012, ApJ, 746, 15
- Bate, M. R. 2009, MNRAS, 392, 590
- Bestenlehner, J. M., Vink, J. S., Gräfener, G., et al. 2011, A&A, 530, L14
- Blaauw, A. 1961, Bull. Astron. Inst. Netherlands, 15, 265
- Bressert, E., Bastian, N., Evans, C. J., et al. 2012, A&A, 542, A49
- Brott, I., de Mink, S. E., Cantiello, M., et al. 2011, A&A, 530, A115
- Cioni, M.-R. L., Clementini, G., Girardi, L., et al. 2011, A&A, 527, A116
- Crowther, P. A., Schnurr, O., Hirschi, R., et al. 2010, MNRAS, 408, 731
- Crowther, P. A., Caballero-Nieves, S. M., Bostroem, K. A., et al. 2016, MNRAS, 458, 624
- Davidson, K., Humphreys, R. M., & Weis, K. 2016, arXiv:1608.02007, arXiv:1608.02007
- de Koter, A., Heap, S. R., & Hubeny, I. 1997, ApJ, 477, 792
- Drew, J. E., Herrero, A., Mohr-Smith, M., et al. 2018, MNRAS, arXiv:1807.06486:1807.06486
- Evans, C. J., Walborn, N. R., Crowther, P. A., et al. 2010, ApJ, 715, L74
- Evans, C. J., Taylor, W. D., Hénault-Brunet, V., et al. 2011, A&A, 530, A108
- Fujii, M. S., & Portegies Zwart, S. 2011, Science, 334, 1380
- Gaia* Collaboration, Brown, A. G. A., Vallenari, A., et al. 2018, ArXiv:1804.09365, arXiv:1804.09365

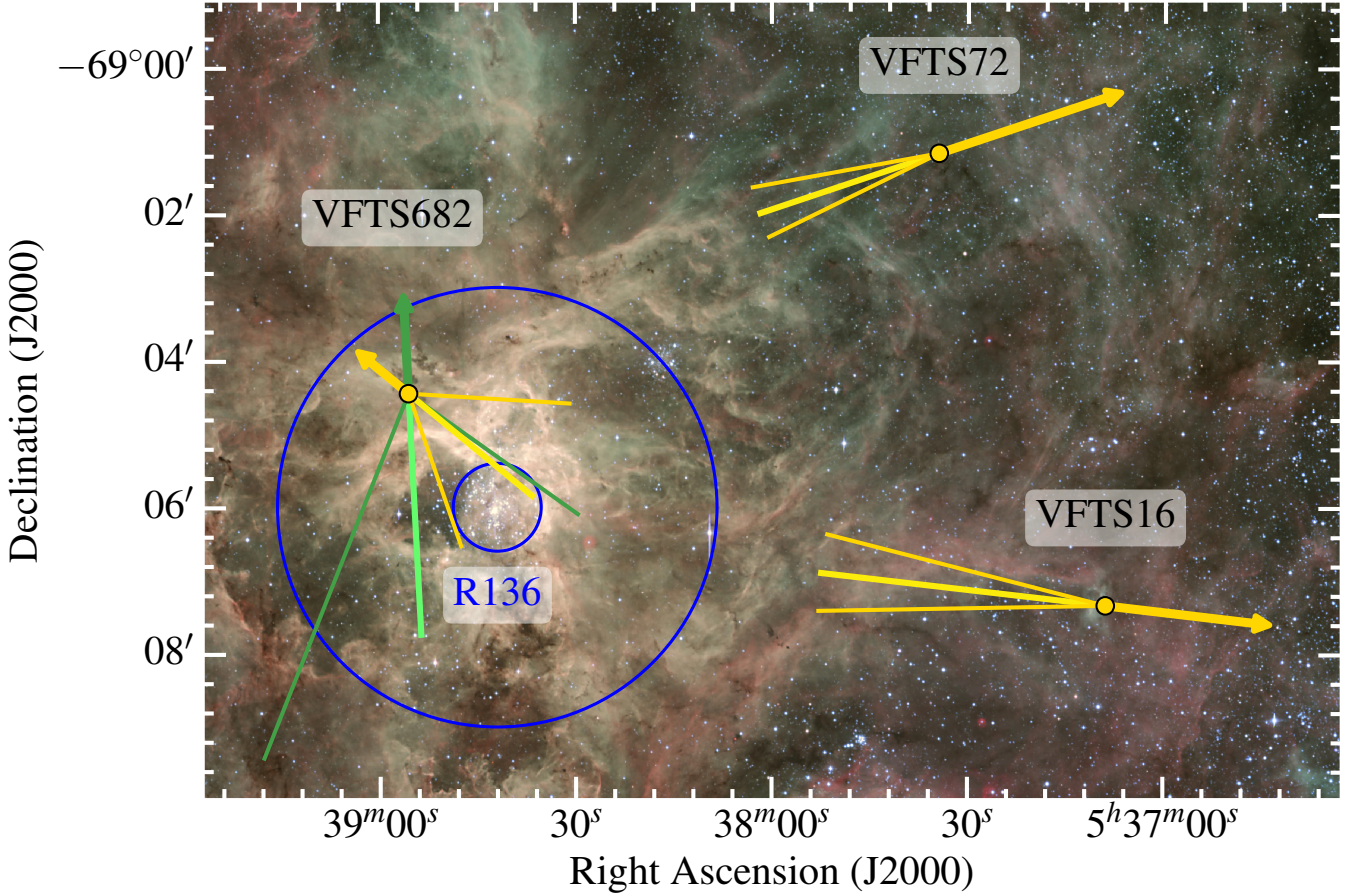


FIG. 2.— The thick yellow arrows indicate proper motions relative R136 (blue circle) from *Gaia* DR2, multiplied by 0.4 Myr. The prolongations in the opposite direction are proportional to the apparent ages of the stars, and the thin lines illustrate the error cone on the potential origin. The green thick arrow indicates the HST proper motion of VFTS682, with the relative error cone and prolongation proportional to its apparent age. The two blue circles indicate the regions of radii 0.01 and 0.05 degrees around the core of R136.

- Gaia Collaboration, Prusti, T., de Bruijne, J. H. J., et al. 2016, *A&A*, 595, A1
 Grasdorf, R. A., & Chu, Y.-H. 2009, *ApJS*, 184, 172
 Gvaramadze, V. V., Weidner, C., Kroupa, P., & Pflamm-Altenburg, J. 2012, *MNRAS*, 424, 3037
 Humphreys, R. M., Weis, K., Davidson, K., & Gordon, M. S. 2016, *ApJ*, 825, 64
 Köhler, K., Langer, N., de Koter, A., et al. 2015, *A&A*, 573, A71
 Kuiper, R., Yorke, H. W., & Turner, N. J. 2015, *ApJ*, 800, 86
 Lada, C. J., & Lada, E. A. 2003, *ARA&A*, 41, 57
 Lamb, J. B., Oey, M. S., Segura-Cox, D. M., et al. 2016, *ApJ*, 817, 113
 Langer, N., Norman, C. A., de Koter, A., et al. 2007, *A&A*, 475, L19
 Lennon, D. J., Evans, C. J., van der Marel, R. P., et al. 2018, *ArXiv:1805.08277*, arXiv:1805.08277
 Luks, T., & Rohlfs, K. 1992, *A&A*, 263, 41
 Meixner, M., Gordon, K. D., Indebetouw, R., et al. 2006, *AJ*, 132, 2268
 Oh, S., & Kroupa, P. 2016, *A&A*, 590, A107
 Pietrzyński, G., Graczyk, D., Gieren, W., et al. 2013, *Nature*, 495, 76
 Platais, I., van der Marel, R. P., Lennon, D. J., et al. 2015, *AJ*, 150, 89
 Platais, I., Lennon, D. J., van der Marel, R. P., et al. 2018, *ArXiv:1804.08678*, arXiv:1804.08678
 Poveda, A., Ruiz, J., & Allen, C. 1967, *Boletín de los Observatorios Tonantzintla y Tacubaya*, 4, 86
 Rakavy, G., & Shaviv, G. 1967, *ApJ*, 148, 803
 Renzo, M., Zapartas, E., de Mink, S. E., et al. 2018, *ArXiv:1804.09164*, arXiv:1804.09164

AFFILIATIONS

- ¹Astronomical Institute Anton Pannekoek, University of Amsterdam, 1098 XH Amsterdam, The Netherlands
²ESA, European Space Astronomy Centre, Apdo. de Correos 78, E-28691 Villanueva de la Cañada, Madrid, Spain

- Rosen, A. L., Krumholz, M. R., McKee, C. F., & Klein, R. I. 2016, *MNRAS*, 463, 2553
 Rubio-Díez, M. M., Najarro, F., García, M., & Sundqvist, J. O. 2017, in IAU Symposium, Vol. 329, The Lives and Death-Throes of Massive Stars, ed. J. J. Eldridge, J. C. Bray, L. A. S. McClelland, & L. Xiao, 131–135
 Sabbi, E., Lennon, D. J., Gieles, M., et al. 2012, *ApJ*, 754, L37
 Sabbi, E., Anderson, J., Lennon, D. J., et al. 2013, *AJ*, 146, 53
 Schneider, F. R. N., Castro, N., Fossati, L., Langer, N., & de Koter, A. 2017, *A&A*, 598, A60
 Schneider, F. R. N., Sana, H., Evans, C. J., et al. 2018, *Science*, 359, 69
 Smith, N. 2016, *MNRAS*, 461, 3353
 Smith, N., & Tombleson, R. 2015, *MNRAS*, 447, 598
 Townsley, L. K., Broos, P. S., Feigelson, E. D., Garmire, G. P., & Getman, K. V. 2006, *AJ*, 131, 2164
 Udalski, A., Soszyński, I., Szymański, M. K., et al. 2008, *Acta Astron.*, 58, 329
 Walborn, N. R., Barbá, R. H., & Sewilo, M. M. 2013, *AJ*, 145, 98
 Ward, J. L., & Kruijssen, J. M. D. 2018, *MNRAS*, 475, 5659
 Zapartas, E., de Mink, S. E., Izzard, R. G., et al. 2017, *A&A*, 601, A29
 Zinnecker, H., & Yorke, H. W. 2007, *ARA&A*, 45, 481

³ Department of Physics & Astronomy, Johns Hopkins University, Baltimore, MD 21218, USA

⁴ Space Telescope Science Institute, 3700 San Martin Drive, Baltimore, MD 21218, USA

⁵Department of Physics and Astronomy, Hicks Building, Hounsfield Road, University of Sheffield, Sheffield S3 7RH,

UK

⁶UK Astronomy Technology Centre, Royal Observatory Edinburgh, Blackford Hill, Edinburgh, EH9 3HJ, UK

⁷ National Research Council, Herzberg Astronomy & Astrophysics, 5071 West Saanich Road, Victoria, BC, V9E 2E7, Canada

⁸ School of Astronomy & Space Science, University of the Chinese Academy of Sciences, Beijing 100012, China

⁹ National Astronomical Observatories, Chinese Academy of Sciences, Beijing 100012, China

¹⁰ Argelander-Institut für Astronomie, Universität Bonn, Auf dem Hügel 71, 53121, Bonn, Germany

¹¹ Centro de Astrobiología, CSIC-INTA, Carretera de Torrejón a Ajalvir km-4, E-28850 Torrejón de Ardoz, Madrid, Spain

¹² Institute of Astronomy, KU Leuven, Celestijnenlaan 200 D, B-3001 Leuven, Belgium

¹³ Department of Physics, University of Oxford, Keble Road, Oxford OX1 3RH, UK

¹⁴ Armagh Observatory, College Hill, Armagh BT61 9DG, UK

We are grateful to J. Heyl, M. C. Ramirez-Tannus, S. N. Shore, and S. Torres for help and discussions, European Unions Horizon 2020 research and innovation programme from the European Research Council (ERC), Grant agreement No. 715063 [SdM], the NRC-Canada Plaskett Fellowship [VHB].

This work has made use of data from the European Space Agency (ESA) mission *Gaia* (<https://www.cosmos.esa.int/gaia>), processed by the *Gaia* Data Processing and Analysis Consortium (DPAC, <https://www.cosmos.esa.int/web/gaia/dpac/consortium>). Funding for the DPAC has been provided by national institutions, in particular the institutions participating in the *Gaia* Multilateral Agreement.